Supporting information for: Optical and electrical excitation of hybrid guided modes in an organic nanofiber-gold film system

Benoît Rogez,[†,¶] Rebecca Horeis,[‡] Eric Le Moal,[*,†] Jens Christoffers,[‡] Katharina Al-Shamery,[‡] Gérald Dujardin,[†] and Elizabeth Boer-Duchemin[†]

Institut des Sciences Moléculaires d´Orsay, CNRS - Université Paris-Sud (UMR 8214), Orsay, France, and Institut für Chemie & Center of Interface Science, Universität Oldenburg, 26129 Oldenburg, Germany

E-mail: eric.le-moal@u-psud.fr

Phone: +33 1 69 15 66 97. Fax: +33 1 69 15 67 77

[*]To whom correspondence should be addressed

[†]ISMO, Orsay, France

[‡]University of Oldenburg, Germany

[¶]Now at: Ludwig-Maximilians-Universität München, Department of Cellular Physiology, München, Germany.

Sample properties and preparation

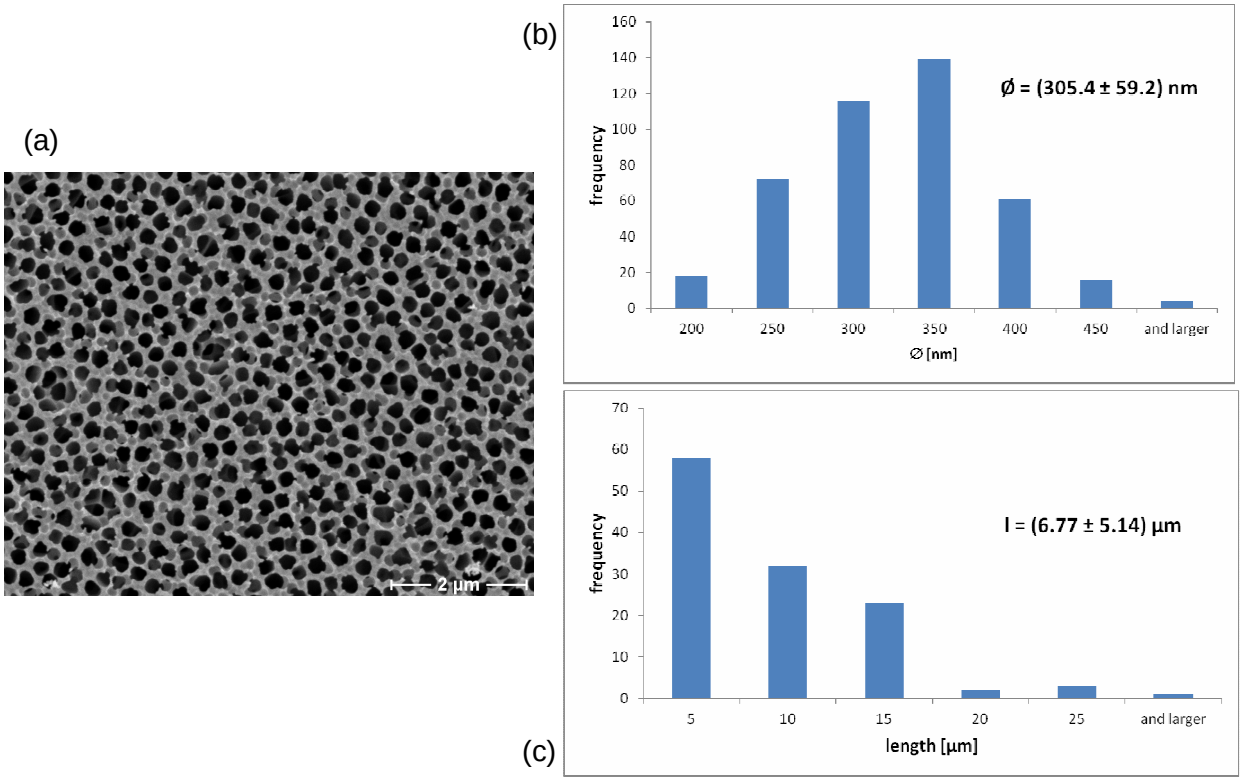

Figure S1: Synthesis and characterization of the organic nanofibers. (a) Scanning electron micrograph of a nanoporous alumina matrix with average pore sizes of 300 nm. (b,c) Histograms of the measured diameter and length distributions of the organic nanofibers (mean value and standard deviation are given in inset).

Photoluminescence of a single nanofiber on gold

Figure S2 shows real-space fluorescence images of a single organic nanofiber on a thin gold film. One can see both the direct light emission through the gold film (at the location of the nanofiber) and leakage radiation of the SPPs propagating away from the nanofiber in these images. Parts (b-g) of the figure are obtained by placing different bandpass filters in front of the detector (central wavelength and width shown in the bottom lefthand corner of each image).

Figure S2h shows an intensity profile taken from the image in Fig. S2f along a line orthogonal to the nanofiber axis, plotted on a semi-log scale. The intense emission peak at the nanofiber position is the photoluminescence of the nanofiber whereas the emission extending up to 40 μm away from the nanofiber is the propagating SPP leakage radiation. From the analysis of such curves, we find that the intensity decays mono-exponentially with distance from the fiber. In Fig. S3a, we plot the decay lengths determined from the mono-exponential fits of intensity profiles for different detection wavelengths (central wavelength of the bandpass emission filters). These decay lengths are in good agreement with the theoretical SPP propagation lengths at the air|gold interface of a 50-nm gold film on glass.[S1,S2] Moreover, we measure that the spectral distribution of the SPP leakage radiation is similar to that of the direct emission from the nanofiber (yet with the attenuation of the high-energy components due to propagation losses, see Fig. S3b). Together, this confirms that SPPs are launched from the nanofiber by the coupling of the nanofiber fluorescence into SPPs. Still, the launching of SPPs on the gold film from the nanofiber may occur through two different ways: direct energy transfer from excited molecules to SPPs or out-coupling of guided modes into SPPs. Furthermore, the out-coupling of guided modes into SPPs may also occur differently: either by coupling of a guided mode to an SPP with conservation of the in-plane wavevector component (i.e. their dispersion curves must overlap) or by scattering of a guided mode at one end of the nanofiber (scattering at a subwavelength structure loosens the condition on momentum conservation). Distinguishing these different mechanisms is difficult, however.

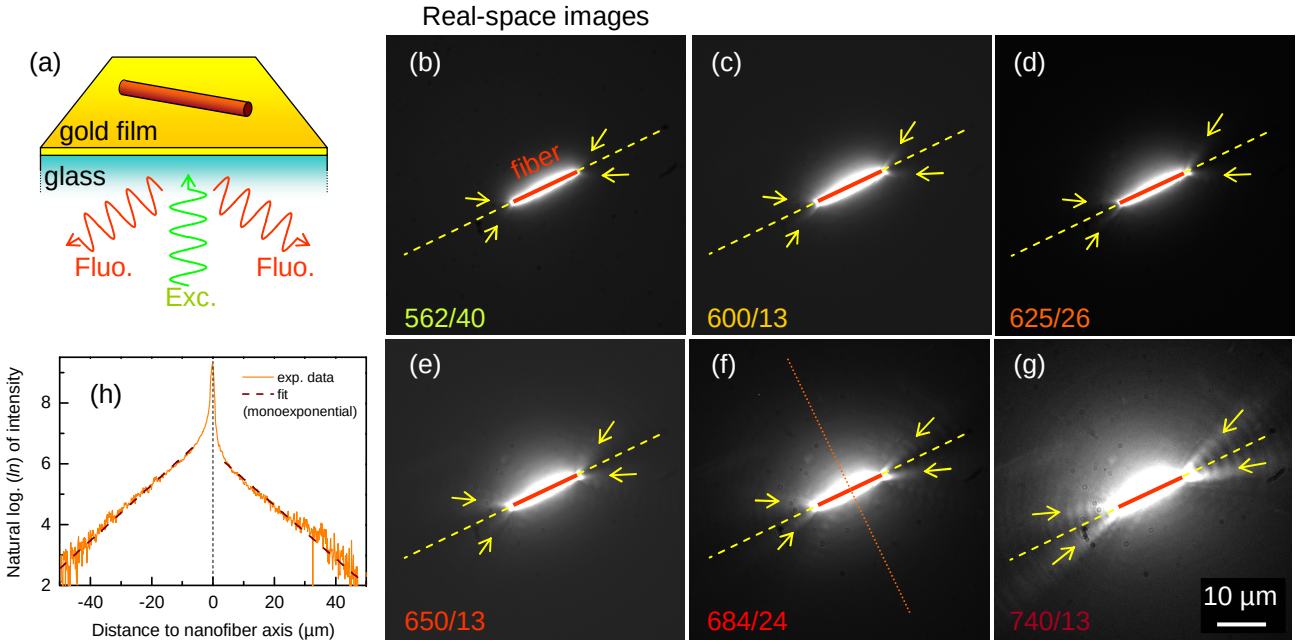

Figure S2: Fluorescence of a single organic nanofiber on a thin gold film (50 nm) upon optical excitation with a Hg lamp (bandpass excitation filter at 488/10 nm). (a) Sketch of the excitation/emission geometry. (b-g) Grey-scale fluorescence images in real space (longpass dichroic mirror starting at 525 nm, microscope objective of NA = 1.45), measured using different bandpass emission filters: (b) 562/40 nm, (c) 600/13 nm, (d) 625/26 nm, (e) 650/13 nm, (f) 684/24 nm, (g) 740/13 nm. The dashed yellow line indicates the fiber axis. The arrows highlight preferential directions of fluorescence out-coupling into surface plasmon polaritons (SPPs). (h) Intensity profile taken from image (f) along the dotted red line and plotted as $\ln I$ versus the distance to the nanofiber axis. This data shows good agreement with a mono-exponential decay fit (dashed black lines).

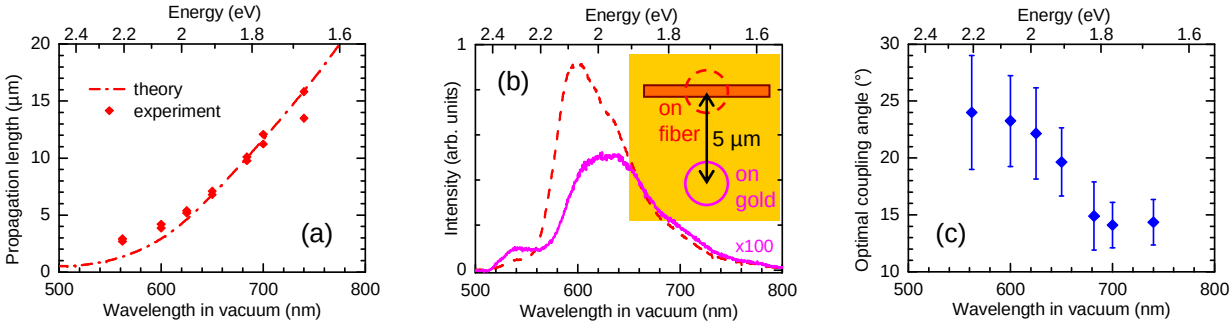

Figure S3: Fluorescence out-coupling into SPPs. (a) Experimental and theoretical propagation lengths of the SPPs launched on the gold film from the organic nanofiber as a function of the emission wavelength in vacuum λ_0 (analysis of the real-space images shown in Fig. S2). Experimental values are determined from a mono-exponential fit of the intensity profile along the perpendicular cross-section of the nanofiber. Theoretical values are calculated for SPPs propagating at the air|gold interface of a 50-nm gold film on glass.[S1,S2] (b) Spectra (optical excitation with a Hg lamp, bandpass excitation filter at 488/10 nm, longpass dichroic mirror starting at 525 nm) from two different areas on the sample (each area is 2 μm in diameter, selected by spatial filtering with an optical fiber). One area is centered on the organic nanofiber (dashed line) and the other is centered on the gold film at a distance of 5 μm from the nanofiber axis (solid line, intensity multiplied by 100). (c) Optimal angle of fluorescence out-coupling into SPPs *versus* the emission wavelength in vacuum. The most intense SPP emission at the fiber end (as indicated by arrows in Figs. S2b-g) is emitted at this optimal angle measured with respect to the axis of the organic nanofiber.

We observe in the real-space images of Fig. S2 that SPP emission from the nanofiber ends occurs in preferential directions, forming a symmetrical V-shaped pattern at each end (see arrows in Fig. S2b-g). This may reveal a strong dependence on angle of the guided mode scattering efficiency at the nanofiber ends; yet, this may also result from the interference between SPPs launched through the different ways mentioned above. As shown in Fig. S3c, the optimal out-coupling angle of the nanofiber fluorescence into SPPs depends on the wavelength and varies within the investigated spectral range from 24° to 14° with respect to the nanofiber axis.

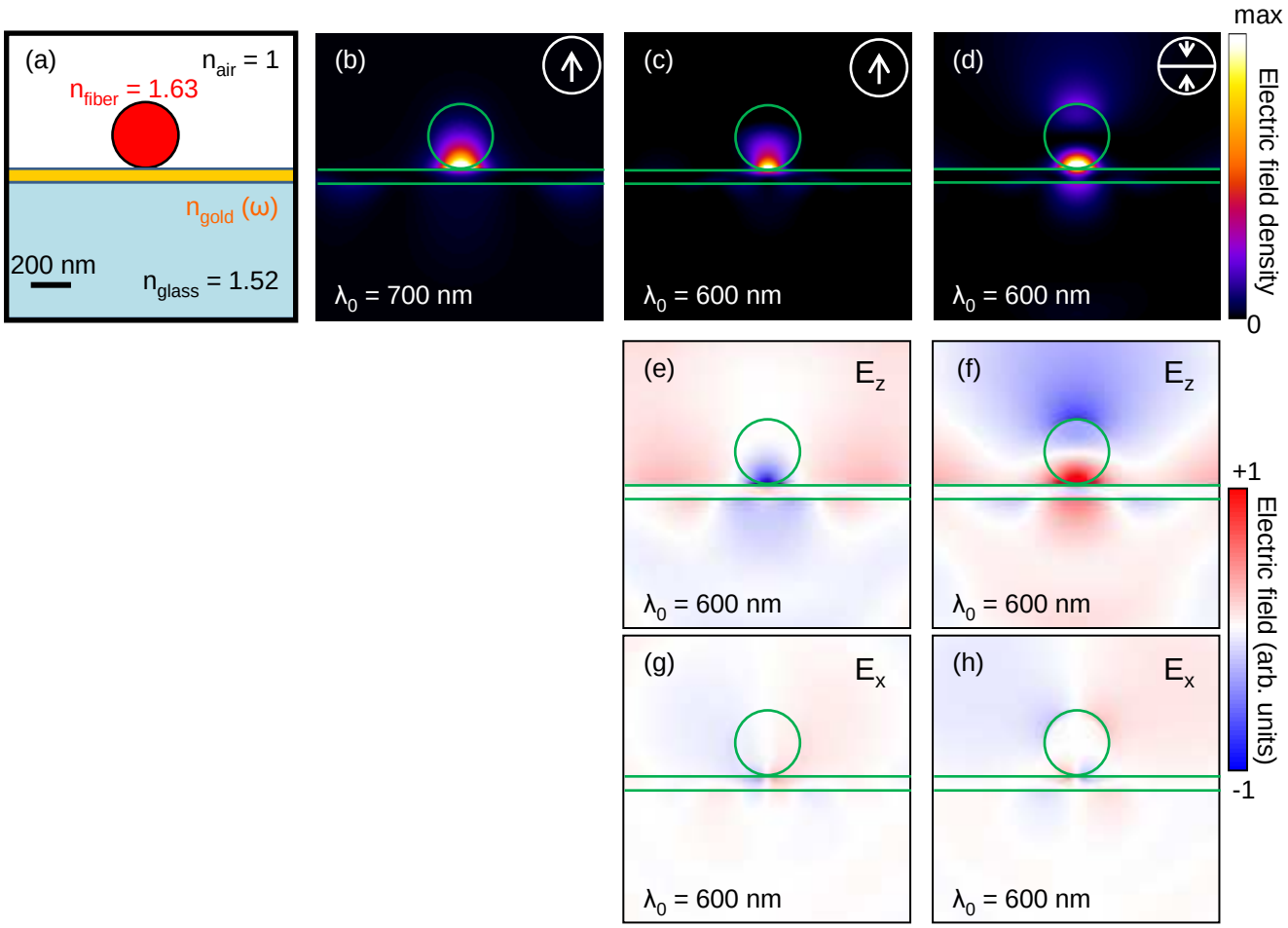

Figure S4: Identification of the guided modes in the organic-nanofiber-on-gold-film system, as derived from finite-difference time-domain (FDTD) calculations. Parts (a-d) are reproduced from the main text for completeness. The electric field components along the z and x-axes are shown in parts (e,f) and (g,h), respectively, for $\mathcal{E} = 2.07$ eV only. Comparing (e) and (g), then (f) and (h), we see that the E_x intensity is basically zero inside the fiber, confirming that the electric field orientation is mainly in the z direction. The lack of red color inside the fiber in (e) and the distinct red and blue areas in part (f) confirm the polarization suggested in the upper righthand corners of parts (c,d). All FDTD calculations are performed using the free software MEEP.[S4]

Coupling an electrical SPP nanosource to a nanofiber on gold

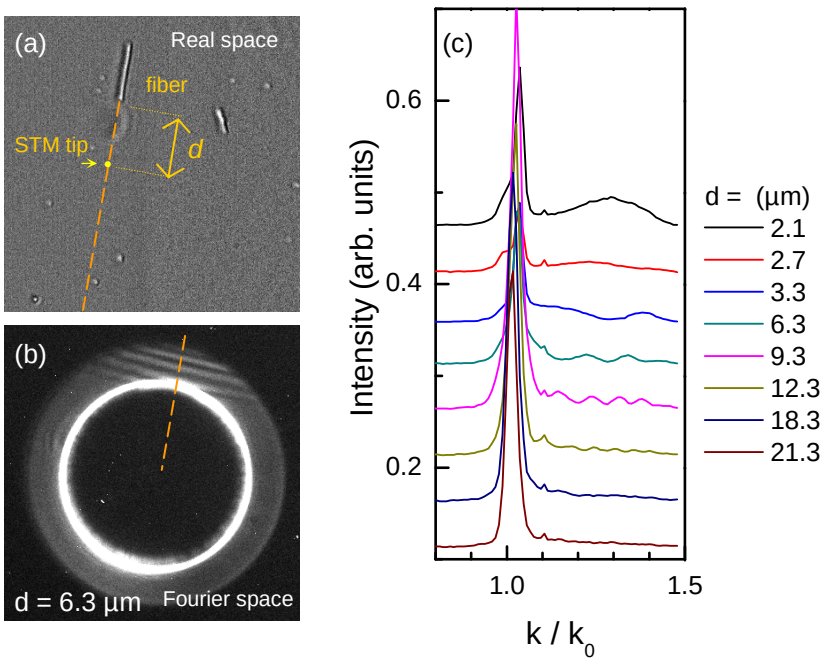

Figure S5: Scattering of electrically excited SPPs at an organic nanofiber on a gold film. (a) Transmission optical image of an organic nanofiber. (b) Grey-scale optical image in Fourier space, measured upon the electrical excitation of SPPs with the STM tip located along the fiber axis, at distance $d = 6.3\mu$m from the fiber end as indicated in (a). (c) Intensity profiles taken from Fourier space images such as those in Fig. 8 in the main text (cross-section obtained along the dotted line as shown in b) measured for different tip-to-fiber distances. The sample is biased to 2.5 V and the tunnel current setpoint is 1 nA. Optical image acquisition time is 300 s. The full emission spectrum is used.

References

(S1) Raether, H. *Surface Plasmons on Smooth and Rough Surfaces and on Gratings*; Springer Tracts in Modern Physcis; Springer-Verlag, Berlin, 1988; Vol. 111.

(S2) Wang, T. Excitation électrique de plasmons de surface avec un microscope à effet tunnel. Ph.D. thesis, Université Paris-Sud, 2012.

(S3) Rakić, A. D.; Djurišić, A. B.; Elazar, J. M.; Majewski, M. L. Optical properties of

metallic films for vertical-cavity optoelectronic devices. *Appl. Opt.* **1998**, *37*, 5271–5283.

(S4) Oskooi, A. F.; Roundy, D.; Ibanescu, M.; Bermel, P.; Joannopoulos, J. D.; Johnson, S. G. Meep: A flexible free-software package for electromagnetic simulations by the FDTD method. *Comput. Phys. Commun.* **2010**, *181*, 687 – 702.